International Journal of Design & Nature and Ecodynamics
Vol. 19, No. 5, October, 2024, pp. 1491-1499
Journal homepage: http://iieta.org/journals/ijdne

Influence of Italian Climatic Conditions on Performance of a 3D Printed Building Second-Skin Façade with 20% Gyroid Filling: Simulation Assessment

Luigi Tufano[1*], Michelangelo Scorpio[1], Benito Andreozzi[1], Alfonso Carola[2], Marco Donisi[2], Antonio Rosato[1], Giovanni Ciampi[1]

[1] Department of Architecture and Industrial Design, University of Campania Luigi Vanvitelli, Built Environment Control Laboratory RIAS, Aversa 81031, Italy
[2] Cosmind s.r.l., Limatola 82030, Italy

Corresponding Author Email: luigi.tufano@unicampania.it

https://doi.org/10.18280/ijdne.190503

Received: 26 May 2024
Revised: 7 October 2024
Accepted: 15 October 2024
Available online: 29 October 2024

Keywords:
building energy efficiency, TRNSYS, dynamic shading, ventilated façade, additive manufacturing

ABSTRACT

This study evaluates the influence of Italian climatic conditions on the performance of a 3D-printed Second-Skin Façade (SSF) installed as a retrofit action for office buildings. In particular, this paper first evaluates the thermal properties of a 3D-printed ASA (Acrylonitrile Styrene Acrylate) sample using the Hot Disk Thermal Constants Analyser TPS 1000. Then, various case studies, where a Second-Skin Façade is installed using the 3D-printed ASA material as the outer layer, were modeled in the dynamic simulation software TRNSYS 18. The study considers a typical Italian office building in four Italian cities under different climatic zones. The analysis is carried out in terms of primary energy savings, reduction of carbon dioxide equivalent emissions, and visual comfort. The results allowed to estimate the potential benefits with respect to the reference case without the SSF, as well as the performance of the investigated material when integrated in an SSF system upon varying the boundary conditions. The simulation results indicated that the proposed SSF system can reduce the primary energy consumption (up to 17.8%), significantly decrease the equivalent CO_2 emissions (up to 30.8 $t_{CO2,eq}$), and improve the visual comfort (UDI_{useful} values up to 95.4%).

1. INTRODUCTION

According to data from the International Energy Agency (IEA), energy consumption in the EU associated with buildings is about 40% of the world's energy use, and up to 36% of its carbon emissions are presently attributed to buildings [1-3]. In addition, only 3% of buildings in the EU have an efficient building envelope [2], only 1% of the EU's buildings are renovated yearly, and about 35% are over 50 years old [4]. There are two main types of refurbishment actions: passive and active [5, 6]. Active actions prioritize utilizing innovative systems and services to achieve greater efficiency and minimize energy usage. Conversely, passive actions aim to diminish energy requirements over the lifespan of a building to enhance sustainability. These passive strategies may involve external features that substantially decrease the need for cooling or can be incorporated as structural elements (like thermal insulation and windows). Additionally, passive retrofit procedures are typically less intrusive and enable repairs without altering the structure of old buildings [7].

Over the years, the construction industry and the research in building technologies have overcome significant challenges to identify more efficient and sustainable solutions. This led to the development of more durable, lightweight, and eco-friendly innovative materials, to be integrated into the traditional buildings components or used along retrofit actions to maximize their impact [8-14]. Numerous studies have examined the integration of 3D-printed solutions in these processes, focusing mainly on design issues, while neglecting their effects on the energy and environmental performances of the building [10]. Among the retrofit actions, several systems have been proposed to improve energy efficiency, indoor comfort, and sustainability of the current building scenario, focusing particularly on the building's envelope and façade systems due to the influence of these components on the performance and design of the building [8-10]. Solutions like Second-Skin Facade (SSF) systems can be one of the most interesting passive retrofit actions, thanks to their lower impact on the existing structure and design flexibility [11, 13, 15]; indeed, appropriate design of SSF systems can positively impact the energy, environment, and economic performances of the building, while also allowing the easy integration of new materials and solutions [16, 17]. In this study, the thermophysical characteristics of a 3D-printed sample made of ASA (Acrylonitrile Styrene Acrylate) filament have been experimentally evaluated by means of the Hot Disk Thermal Constants Analyser TPS 1000 [18], widely used for characterizing the thermal properties of an extensive range of materials in a short time [19, 20]. Then, several case studies involving the installation of a SSF system that uses the 3D-printed ASA material as the outer layer have been modelled in the dynamic simulation software TRNSYS 18 [21]. A typical Italian office building has been considered as a reference case

located in four Italian cities (which differ in terms of heating degrees days (HDD), i.e., Palermo, Napoli, Pisa, and Milano, carrying out an analysis in terms of primary energy saving, reduction of carbon dioxide equivalent emissions, and visual comfort. The performance of such material when integrated in a SSF system upon varying the boundary conditions have been evaluated in comparison to the reference case without the SSF.

2. MATERIALS AND METHODS

In this section, the procedures and results for the experimental characterization of the 3D-printed sample are described, together with the details of the TRNSYS simulation models and the methodology for the energy, environmental and visual analyses.

2.1 Material characterization

The analyzed sample consists of a couple of identical 3D-printed specimens, two disks with a diameter of 6 cm and a thickness of 1.5 cm, made of ASA (Acrylonitrile Styrene Acrylate), a UV-resistant 3D-printable plastic polymer [22]. The sample was realized by using the 3D printer Stratasys F900 with the Fused Deposition Modeling (FDM) technology [23], considering a 20% Gyroid filling. The dimensions of the specimens were defined considering the guidelines suggested by the manufacturer of the Hot Disk Thermal Constants Analyser (TPS 1000) [18] used to measure the thermal conductivity, the thermal diffusivity and the volumetric specific heat of the sample through the Transient Plane Source (TPS) method [24]: in particular, considering the radius of the sensor (r_{sensor}= 1.5 cm), a bifilar nickel spiral sealed in a thin film of Kapton tape, the specimens have been realized considering the minimum and maximum suggested thickness (minimum=r_{sensor}; maximum=2*r_{sensor}) and diameter (minimum=3*r_{sensor}; maximum=4*r_{sensor}), in order to minimize the variances caused by the anisotropy of the 3D-printed geometries and the edge effects [25]. The infill percentage of 20% was set considering the results of previous studies [20, 26-28].

The measurements were carried out in the RIAS Laboratory of the Department of Architecture and Industrial Design of the University of Campania Luigi Vanvitelli [29].

During the measurements, the sensor is stacked between the two identical 3D-printed specimens, and then a small electrical current (90 mW) is applied during a test time (640 s) correlated to the thermal diffusivity of the sample. The heat generated by the sensor diffuses into the sample at a rate dependent on the thermal transport characteristics of the material. The time-dependent temperature increase in the sensor (ΔT) is recorded during the test, which allows resolving l, α and c_p of the material by iterative fitting to the corresponding mathematical model [24, 30]. The measurements were performed under controlled boundary conditions (ambient temperature = 23 ± 2°C, and relative humidity = 50 ± 10%) monitored via a Pt100 thermocouple and covering the samples with a steel cover to avoid a temperature drift. Between two consecutive measurements, a long relaxation time has been accounted to let the setup reach thermal equilibrium [18].

Figure 1 shows the two specimens clamped in the TPS 1000, with the sensor in-between and the Pt100 thermocouple on the side.

Figure 1. The sample set in the TPS 1000 without the steel cover

The measured thermal properties of the ASA 3D-printed sample are reported in Table 1.

Table 1. Thermal properties of the sample

Parameter	Value
Thermal conductivity	0.0249 W/mK
Thermal diffusivity	0.0217 mm^2/s
Volumetric specific heat	1.13 MJ/m^3K

2.2 Simulation model

The simulation study has been carried out in four different Italian cities to evaluate the performance of the proposed 3D-printed solution when integrated into a SSF upon varying climatic conditions. In particular, the four considered cities are: Palermo (38°06′56.37″N 13°21′40.54″E, HDD=751), Napoli (40°50′09″N 14°14′55″E, HDD=1034), Pisa (43°43′N 10°24′E, HDD=1694), and Milano (45°28′01″N 9°11′24″E, HDD =2404). The office building is modelled referencing a typical office structure from IEA Annex 27 activities [31] and consists of 7 floors, each having a floor space of 661 m^2 and a height of 4.13 m. The geometrical model was realized using SketchUp 3D-modeling software, dividing each floor into five thermal zones (TZ) upon varying the space typology, office (Of1 and Of2) or stairs (St), and the orientation, east (E) or west (W). Figure 2 reports an axonometric view of the reference office building model, while Figure 3 shows the third-floor plan as an example of the TZ subdivision per floor.

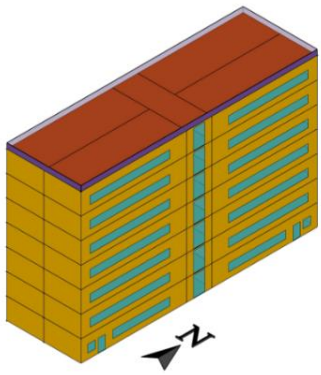

Figure 2. Axonometric view of the building model and the TZ subdivision

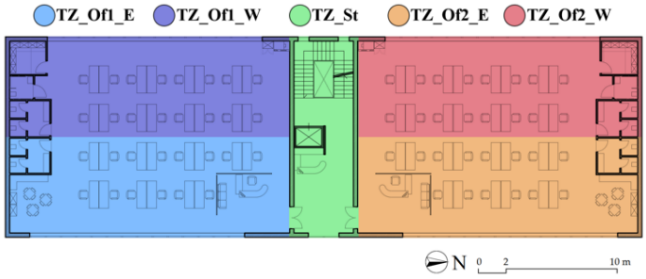

Figure 3. Scheme of the thermal zone division per floor

Each floor has continuous windows on the east and west facades, sized based on the appropriate Windows-to-Wall Ratio (WWR) for each orientation [32]. The WWR ratios of the east and west façades are equal to 33% and 34%, respectively. TRNSYS Type 56 is used to import the geometric model in TRNSYS 18 and define in detail the building envelope, the internal gains (people, equipment, and artificial lighting systems), and the target value for cooling and heating systems.

Table 2 outlines the simulation parameters common to all the simulation cases in this study, namely the occupancy schedule, the temperature setpoint for heating and cooling, the thermal gains associated with the occupants, lighting systems, and general equipment, and the air infiltration rate [32-36].

Table 2. Common simulation parameters

Parameter	Value
Occupancy	08:00-17:00 (vacant during w/e)
Temperature setpoint, winter	20°C (occupied) / 15°C (vacant & stairs)
Temperature setpoint, summer	26°C (occupied) / 29°C (vacant & stairs)
Lighting system	12.5 W/m^2 (occupied) / 0.0 W/m^2 (vacant)
Equipment	10.0 W/m^2 (occupied) / 1.0 W/m^2 (vacant)
People	7.0 W/m^2 (occupied) / 0.0 W/m^2 (vacant)
Air infiltration rate	0.6 m^3/h

The thermal transmittance (U-value) of the opaque and transparent surfaces of the building envelope was defined according to Schimschar et al. [37]. Considering the characteristics of buildings constructed during the 1980-90 decades, the construction typology most common in the country and in need of renovation [37]. In particular, the following U-values for the reference building were used: 0.80 W/m^{2}K for vertical walls and roof, 0.50 W/m^{2}K for the floor, and 4.20 W/m^{2}K for the window.

For the refurbishment of the building, a SSF system has been installed on all the exterior walls of the reference building. The SSF system comprises an outer layer made of 3D-printed ASA panels, a 10 cm air cavity, and an insulation layer. The thickness of the insulation layer (Expanded Polystyrene - EPS, l = 0.041 W/mK) has been set differently to reach the U-value threshold suggested by the Italian legislation for each climatic zone [38].

The SSF system is implemented in TRNSYS through the Type 1230, which simulates the performance of the SSF system by taking into account the following factors: (i) solar radiation, longwave radiation and air convection on the external surface of the outside layer; (ii) thermal stored energy and conduction in the outside layer; (iii) radiation exchange between the outside layer and the air cavity; (iv) convective exchanges from all the surfaces facing the air cavity; (v) conduction through the interface layer [39].

The thermal conductivity of the 3D-printed ASA panels has been set equal to 0.0249 W/mK, as returned by the experimental results, while the panel thickness has been assumed equal to 1 cm. Two variations of the ASA panels have been considered to be installed on the opaque and transparent surfaces of the building's envelope: full panel (Figure 4(a)) and perforated panel with a porosity of 28% [10, 16]. The perforated panels can be moved to cover or uncover the windows (Figure 4(b)) with independent control for each thermal zone based on the incident vertical solar irradiation threshold (50 W/m^2) on the façades.

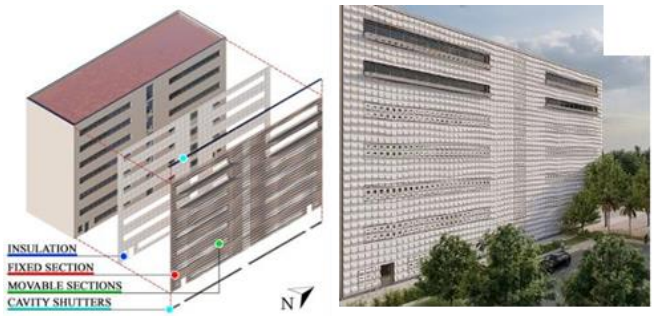

(a) (b)

Figure 4. (a) Building model with a schematic view of the proposed SSF, (b) Model of the dynamic shading system

Figure 5 reports the layout of the 34 horizontal illuminance measurement points placed at 0.80 m height from the floor to evaluate visual comfort on each story.

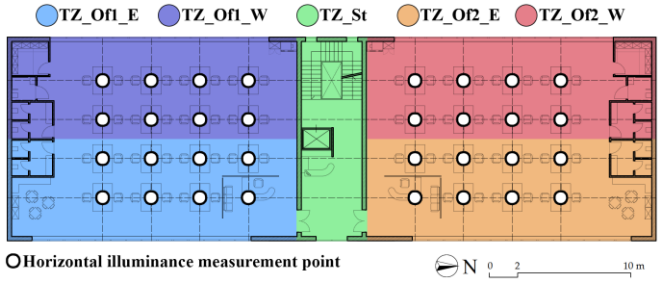

Figure 5. Layout of the illuminance measurement points

The SSF system is provided with shutters at the air cavity's inlet and outlet, controlled to keep the cavity open only when the outdoor air temperature is higher than 20°C to maximize natural inner ventilation. Table 3 summarizes all the simulation case studies, including the specific characteristics of the electric air-to-air vapor compression heat pumps (EHPs) for the offices' zones [35], the insulation thicknesses, and the U-values.

Table 3. Summary of the simulation case studies

City	EHP in the Offices	SSF Installed	Ins. Thick. (m)	U-value (W/m^{2}K)
Palermo	COP: 2.81	No	-	0.80
	EER: 2.78	Yes	0.020	0.40
Napoli	COP: 2.63	No	-	0.80
	EER: 2.46	Yes	0.032	0.36
Pisa	COP: 2.63	No	-	0.80
	EER: 2.46	Yes	0.046	0.32
Milano	COP: 2.77	No	-	0.80
	EER: 2.67	Yes	0.064	0.28

Whatever the location of the simulation cases, the thermal zones of the stairs are served by the same EHPs with COP equal

to 2.62 and EER equal to 2.75 [35].

2.3 Energy, environmental and visual analysis

The analysis of energy consumption involves assessing primary energy usage, which is determined by evaluating the Primary Energy Saving (PES) as reported in the study by Carlucci et al. [40].

$$\mathrm{PES} = \left(1 - \frac{E_{el,B}^{PC}/\eta PP}{E_{el,B}^{RR}/\eta PP}\right) \cdot 100 \qquad (1)$$

where, $E_{el,B}^{RC}$ represents the overall electric energy consumed by the reference cases (RC) and associated to the operation of equipment, lighting systems, EHPs, while $E_{el,B}^{PC}$ is the overall electric energy associated to the proposed cases (PC) and due to the operation of equipment, lighting systems, EHPs, and η_{PP} is the power plants' average efficiency assumed equal to 0.465 [28]. A positive PES index indicates that the implemented passive retrofit measures reduce primary energy consumption in comparison to the reference case.

The environmental comparison is conducted by assessing the reduction of carbon dioxide equivalent emissions (ΔCO_2), defined according to Herzanita et al. [14] and reported below:

$$\Delta CO_2 = m_{CO_2,eq}^{RC} - m_{CO_2,eq}^{PC} = \alpha \cdot \left(E_{el,B}^{RC} - E_{el,B}^{PC}\right) \qquad (2)$$

where, $m_{CO_2,eq}^{RC}$ represents the mass of carbon dioxide equivalent emissions for the reference cases and $m_{CO_2,eq}^{PC}$ represents the mass of carbon dioxide equivalent emissions for each of the four proposed cases, and α is the carbon dioxide equivalent emission factor linked to electricity production in Italy and assumed equal to 0.324 $kgCO_{2,eq}/kWh_{el}$ [28]. Consequently, ΔCO_2 index signifies the capacity of the implemented passive retrofit measures to decrease the carbon dioxide equivalent emissions in the renovated case compared to the reference case.

Visual comfort has been evaluated considering the Continuous Daylight Autonomy (CDA) and the Useful Daylight Illuminance (UDI) [40]. The CDA represents the amount of natural light available at a given point of the space during occupied hours with an illuminance value equal to 300 lux:

$$\mathrm{CDA} = \frac{\sum_i (wf_1 \cdot t_i)}{\sum_i t_i} \epsilon [0,1] \qquad (3)$$

$$\text{with } wf_i = \begin{cases} 1 & \text{if } E_{daylight} \geq E_{limit} \\ \frac{E_{daylight}}{E_{limit}} & \text{if } E_{daylight} < E_{limit} \end{cases}$$

where, $E_{daylight}$ is the daylight illuminance calculated at each simulation timestep *i*, and E_{limit} is the illuminance limit equal to 300 lux.

The UDI consists of these three different fractions (Eq. (4)):

$$\mathrm{UDI} = \frac{\sum_i (wf_i \cdot t_i)}{\sum_i t_i} \epsilon [0,1] \begin{cases} UDI_{overlit} \\ \text{with } wf_i = \begin{cases} 1 \text{ if } E_{daylight} > E_{upper\ limit} \\ 0 \text{ if } E_{daylight} \leq E_{upper\ limit} \end{cases} \\ UDI_{useful} \\ \text{with } wf_i = \begin{cases} 1 \text{ if } E_{lower\ limit} \leq E_{daylight} \leq E_{upper\ limit} \\ 0 \text{ if } E_{daylight} < E_{lower\ limit} \vee E_{daylight} > E_{upper\ limit} \end{cases} \\ UDI_{underlit} \\ \text{with } wf_i = \begin{cases} 1 \text{ if } E_{daylight} < E_{lower\ limit} \\ 0 \text{ if } E_{daylight} \geq E_{lower\ limit} \end{cases} \end{cases} \qquad (4)$$

where, t_i is each occupied hour in a year; wf_i is a weighting factor depending on values of $E_{daylight}$ and the illuminance limit value (upper or lower), $UDI_{overlit}$ is the percentage of time of discomfort due to daylight supply, calculated at each simulation timestep i, above the limit (2000 lux), $UDI_{underlit}$ is the percentage of time of discomfort due to daylight supply, calculated at each simulation timestep i, under the limit (100 lux), and UDI_{useful} is the percentage of time with appropriate illuminance levels.

3. RESULTS

This section reports the comparison between the reference cases (RC) and the proposed retrofit cases (PC) from energy, environmental, and indoor visual comfort points of view. Figures 6(a) and 6(b) report the values of PES and ΔCO_2, respectively, as a function of the city.

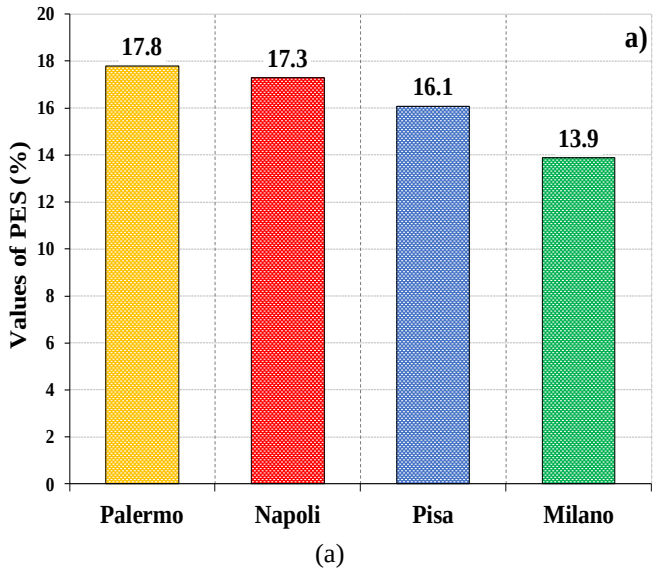

(a)

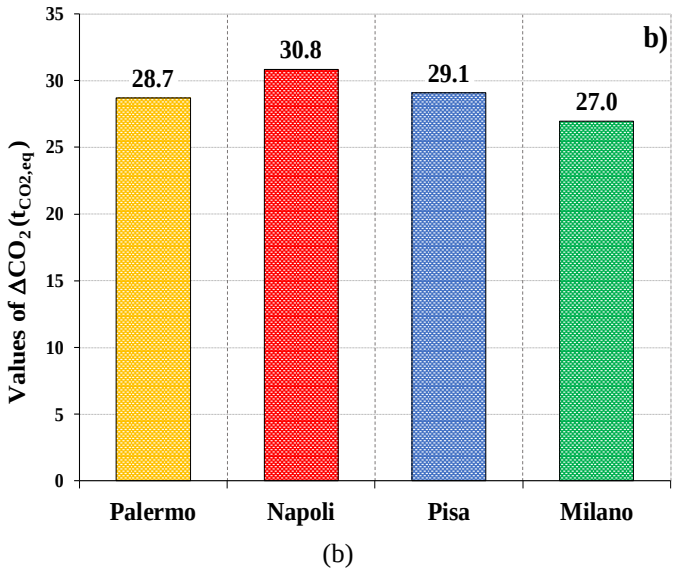

(b)

Figure 6. Values of (a) PES, and (b) ΔCO_2

Table 4. Specific cooling and thermal energy yearly demand for the whole building

Case Study	Cooling Energy Demand Associated with the Whole Building (kWh/m^2/year)	Thermal Energy Demand Associated with the Whole Building (kWh/m^2/year)
RC-Palermo	66.0	8.9
PC-Palermo	36.8	10.1
RC-Napoli	57.7	28.0
PC-Napoli	31.3	25.3
RC-Pisa	48.8	39.4
PC-Pisa	25.5	35.3
RC-Milano	39.7	67.4
PC-Milano	20.8	58.8

Table 5. Summary of visual comfort indices for all case studies

		CDA (%)	UDI_{useful} (%)	$UDI_{underlit}$ (%)	$UDI_{overlit}$ (%)
RC-Palermo	Min.	97.6	20.3	0.8	23.1
	Max	98.9	75.1	1.8	78.8
	Avg.	98.4	37.4	1.2	61.4
	St. dev.	0.4	15.7	0.3	15.9
PC-Palermo	Min.	30.1	46.3	4.0	0.0
	Max	75.7	95.4	53.7	0.6
	Avg.	53.5	82.7	17.2	0.1
	St. dev.	13.34	12.1	12.2	0.2
RC-Napoli	Min.	96.4	24.1	1.7	19.9
	Max	97.8	77.3	2.8	74.1
	Avg.	97.3	43.1	2.3	54.6
	St. dev.	0.4	15.3	0.4	15.7
PC-Napoli	Min.	30.1	44.1	7.2	0.0
	Max	71.6	92.8	55.9	0.0
	Avg.	51.5	77.5	22.5	0.0
	St. dev.	12.2	12.7	12.7	0.0
RC-Pisa	Min.	95.5	30.3	1.5	17.4
	Max	97.8	79.3	3.4	68.2
	Avg.	96.9	47.1	2.2	50.7
	St. dev.	0.7	14.4	0.6	14.9
PC-Pisa	Min.	27.6	38.5	6.6	0.0
	Max	72.2	93.4	61.5	0.0
	Avg.	49.9	75.4	24.6	0.0
	St. dev.	12.9	13.7	13.7	0.0
RC-Milano	Min.	87.6	35.0	2.2	13.7
	Max	96.6	81.6	4.7	62.6
	Avg.	95.1	50.9	3.3	45.8
	St. dev.	1.7	13.8	0.8	14.5
PC-Milano	Min.	26.7	34.0	10.3	0.0
	Max	69.4	89.7	66.0	0.5
	Avg.	48.4	71.4	28.5	0.1
	St. dev.	12.7	13.6	13.6	0.2

Table 4 reports the specific cooling and thermal energy yearly demands associated with the whole office building upon varying the location.

Figure 6 and Table 4 highlight that:

- whatever the city is, the proposed cases allow for a reduction of both the primary energy consumption and the CO_2 equivalent emissions in comparison to the reference cases;
- the values of PES range from a minimum of 13.9% in Milano up to a maximum equal to 17.8% in Palermo;
- the values of ΔCO_2 range from a minimum of 27.0 $t_{CO2,eq}$ obtained when the building is located in Milano up to a maximum equal to of 30.8 $t_{CO2,eq}$ returned when the building is located in Napoli;
- when the building is located in Napoli, the SSF system allows to obtain the best reduction in terms of overall energy demand for both space cooling and heating of -29.0 kWh/m^2/year, while when the building is located in Pisa the proposed system returns the worst reduction in terms of overall energy demand for both space cooling and heating equal to -27.5 kWh/m^2/year;

- the maximum reduction in terms of cooling energy demand is obtained in Palermo (-29.2 kWh/m^2/year), while the minimum reduction in terms of cooling energy demand is achieved when the city is Milano (-18.9 kWh/m^2/year);
- the SSF system allows for a reduction of thermal energy demand for Napoli (-2.6 kWh/m^2/year), Pisa (-4.1 kWh/m^2/year), and Milano (-8.6 kWh/m^2/year), while the proposed system increases the thermal energy demand for Palermo (1.2 kWh/m^2/year).

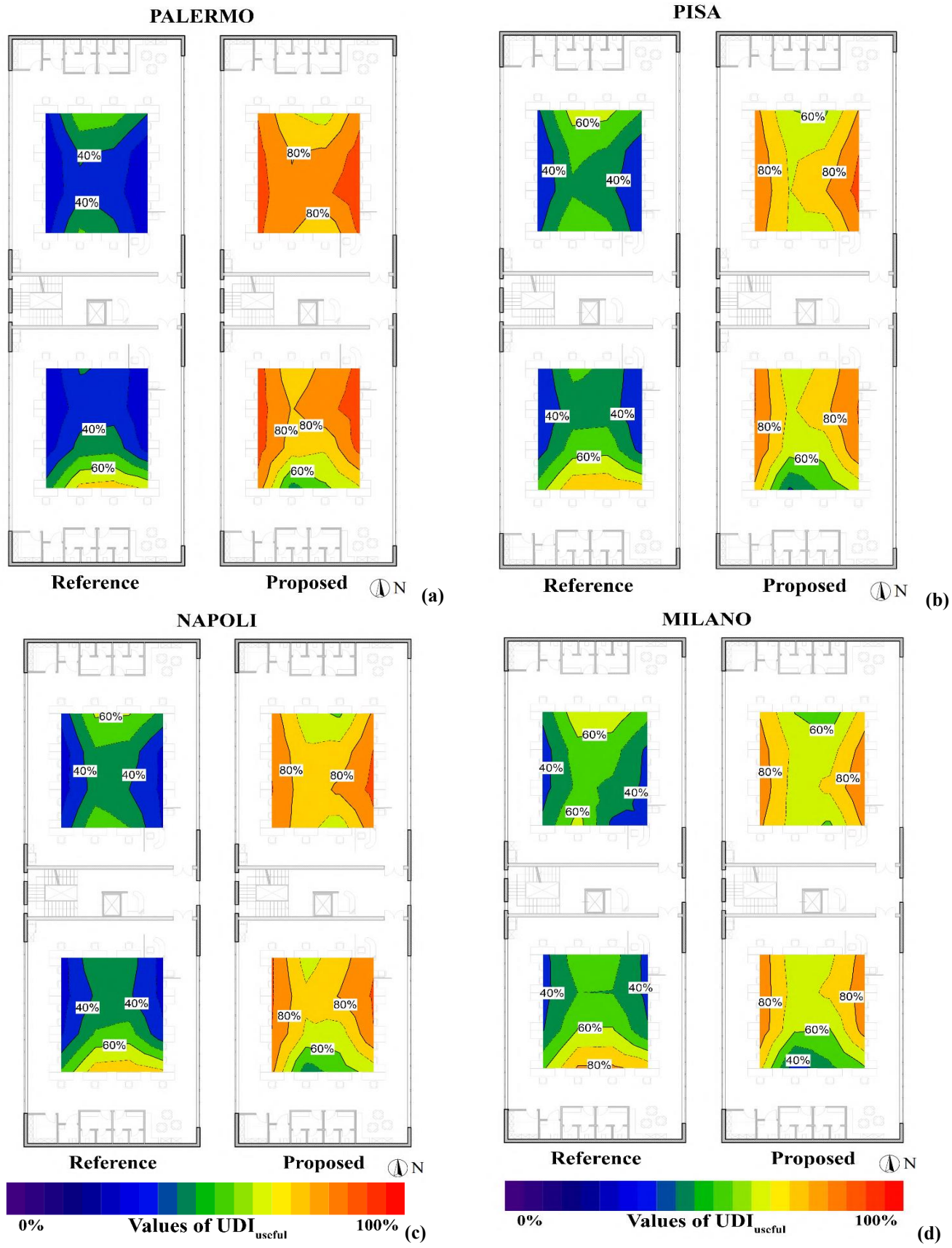

Figure 7. Distributions of UDI_{useful} values at the third floor upon varying the simulation cases: (a) Palermo, (b) Napoli, (c) Pisa, and (d) Milano

Table 5 reports the minimum, maximum, average, and standard deviation values calculated on the third floor of the office building for all cases with reference to the parameters CDA and UDI. Figure 7 reports the values of UDI_{useful} calculated on the third floor.

In terms of indoor visual comfort, Table 5 and Figure 7 show that:

- whatever the city is, the SSF system returned better performance in terms of UDI_{useful} if compared with the RC, although the simulation results showed a reduction of the CDA values;
- the best results in terms of UDI_{useful} are obtained when the building is in Palermo (maximum equal to 95.4%, minimum equal to 46.3%, and average value of 82.7%), while the worst results are returned in Milano (maximum equal to 89.7%, minimum equal to 34.0%, and average value of 71.4%);
- the SSF system returned better results in terms of $UDI_{overlit}$ when compared to the RC, whatever the location is; this means that, during the year, the time of discomfort due to daylight illuminance values above 2000 lux is reduced;
- in contrast to these results, it is important to highlight that the SSF system returned $UDI_{underlit}$ values greater than those returned in RC for all the locations; this means that, during the year, the time with daylight illuminance values under 100 lux is increased; this occurs mainly in the southern area of the building, caused by the used control logic, mainly devoted to the reduction of thermal loads.

The results in terms of indoor visual comfort are similar with reference to all floors of the building.

4. CONCLUSIONS

This study explores the energy, environmental, and visual comfort performances of a SSF system integrating dynamic 3D-printed panels as retrofit action for a typical office building in four Italian cities characterized by different climatic zones. The numerical simulation returned good results in terms of primary energy saving (up to 17.8% in Palermo), reduction of carbon dioxide equivalent emissions (up to 30.8 $t_{CO2,eq}$ in Napoli), and visual comfort (UDI_{useful} values up to 95.4% in Palermo). Future research will focus on further optimizing the characteristics of the 3D-printed panels, particularly their design and operational states. In particular, (i) additional experimental tests of the 3D-printed material upon varying the filling percentage will be carried out, (ii) further optimization of the SSF control logic considering different operation strategies will be developed, and (iii) a 3D-printed panel will be tested in real operating conditions.

ACKNOWLEDGMENT

For the publication of this article, the authors would like to thank: (i) the "Bando di Ateneo per il finanziamento di progetti di ricerca fondamentale ed applicata dedicato ai giovani Ricercatori" of the University of Campania Luigi Vanvitelli (Italy), Project title: "Design and AssessmeNt of innovative Textile and 3D-printEd systems for HUMan-centered spaces"—DANTEHUM, CUP: B63C23000650005, (ii) the Next Generation EU funded PNRR PhD Program, Italian DM 352/2022, CUP: B31J22000450006, mission: "M4C2", investment type and scholarship category: "I.3.3 innovativi", scholarship code: DOT22B2TTX.

REFERENCES

[1] IEA. (2023). Energy Statistics Data Browser – Data Tools. https://www.iea.org/data-and-statistics/data-tools/energy-statistics-data-browser?country=WEOEUR&fuel=Energy%20consumption&indicator=TFCShareBySector, accessed on Oct. 12, 2024.

[2] Corticos, N.D. (2020). Improving residential building efficiency with membranes over façades: The Mediterranean context. Journal of Building Engineering, 32: 101421. https://doi.org/10.1016/j.jobe.2020.101421

[3] Grafkina, M., Sviridova, E., Vasilyeva, E., Vinogradov, O. (2024). Reducing the Concentration of carbon dioxide in indoor air using absorption-based capture. International Journal of Environmental Impacts, 7(2): 197-204. https://doi.org/10.18280/ijei.070205

[4] Energy Performance of Buildings Directive. (2019). New rules for greener and smarter buildings will increase quality of life for all Europeans. https://commission.europa.eu/news/new-rules-greener-and-smarter-buildings-will-increase-quality-life-all-europeans-2019-04-15_en, accessed on Oct. 12, 2024.

[5] Diallo, T.M.O., Zhao, X., Dugue, A., Bonnamy, P., Javier Miguel, F., Martinez, A., Theodosiou, T., Liu, J.S., Brown, N. (2017). Numerical investigation of the energy performance of an Opaque Ventilated Façade system employing a smart modular heat recovery unit and a latent heat thermal energy system. Appl Energy, 205: 130-152. https://doi.org/10.1016/j.apenergy.2017.07.042

[6] Scorpio, M., Ciampi, G., Spanodimitriou, Y., Laffi, R., Rosato, A., Sibilio, S. (2019). Double-skin facades with semi- transparent modules for building retrofit actions: Energy and visual performances. In Proceedings of Building Simulation 2019: 16th Conference of IBPSA, Rome, Italy, pp. 464-471. https://doi.org/10.26868/25222708.2019.210989

[7] Balali, A., Hakimelahi, A., Valipour, A. (2020). Identification and prioritization of passive energy consumption optimization measures in the building industry: An Iranian case study. Journal of Building Engineering. 30: 101239. https://doi.org/10.1016/j.jobe.2020.101239

[8] Ahmed, G.H. (2023). A review of "3D concrete printing": Materials and process characterization, economic considerations and environmental sustainability. Journal of Building Engineering, 66: 105863. https://doi.org/10.1016/J.JOBE.2023.105863

[9] Bedarf, P., Dutto, A., Zanini, M., Dillenburger, B. (2021). Foam 3D printing for construction: A review of applications, materials, and processes. Automation in Construction, 130: 103861. https://doi.org/10.1016/j.autcon.2021.103861

[10] Spanodimitriou, Y., Ciampi, G., Tufano, L., Scorpio, M. (2023). Flexible and lightweight solutions for energy improvement in construction: A literature review. Energies, 16(18): 6637. https://doi.org/10.3390/en16186637

[11] Ascione, F., Bianco, N., Iovane, T., Mastellone, M.,

Mauro, G.M. (2021). The evolution of building energy retrofit via double-skin and responsive façades: A review. Solar Energy. 224: 703-717. https://doi.org/10.1016/J.SOLENER.2021.06.035
[12] Mokhtari, N., Ciampi, G., Spanodimitriou, Y., Sibilio, S. (2023). Second-skin façades and usage of textile materials in the building envelope: Literature review, limitations, and future opportunities. In Proceedings of International Conference on Sustainability in Architecture, Planning, and Design-BEYOND ALL LIMITS 2022, pp. 307-313.
[13] Spanodimitriou, Y., Ciampi, G., Scorpio, M., Mokhtari, N., Teimoorzadeh, A., Laffi, R., Sibilio, S. (2022). Passive strategies for building retrofitting: Performances analysis and incentive policies for the Iranian scenario. Energies, 15(5): 1628. https://doi.org/10.3390/en15051628
[14] Herzanita, A., Lestari, R.T., Dewi, A.P. (2024). Assessing green building implementation and barriers in campus settings. International Journal of Environmental Impacts, 7(3): 591-599. https://doi.org/10.18280/ijei.070320
[15] Mokhtari, N., Ciampi, G., Spanodimitriou, Y., Nocente, A., Manni, M., Lobaccaro, G., Scorpio, M., Sibilio, S. (2023). Textile as second-skin façade for building envelope retrofitting: A numerical analysis on the comfort, energy and environmental impacts in different European climates. In Proceedings of Building Simulation 2023: 18th Conference of IBPSA, Shanghai, China, pp. 1901-1908. https://doi.org/10.26868/25222708.2023.1484
[16] Ciampi, G., Spanodimitriou, Y., Scorpio, M., Rosato, A., Sibilio, S. (2021). Energy performances assessment of extruded and 3D printed polymers integrated into building envelopes for a south Italian case study. Buildings, 11(4): 141. https://doi.org/10.3390/buildings11040141
[17] Hashemi, N., Fayaz, R., Sarshar, M. (2010). Thermal behaviour of a ventilated double skin facade in hot arid climate. Energy and Buildings, 42(10): 1823-1832. https://doi.org/10.1016/j.enbuild.2010.05.019
[18] HOT DISK: TPS 1000. (2024). https://www.hotdiskinstruments.com/products/instruments/tps-1000, accessed on Oct. 12, 2024.
[19] Rosato, A., El Youssef, M., Bashir, M., Daoud, H. (2024). Experimental analysis of thermal properties of tuff from the Campania region in Italy for the design and performance assessment of ground energy systems. In: For Nature/With Nature: New Sustainable Design Scenarios, pp. 571-589. https://doi.org/10.1007/978-3-031-53122-4_35
[20] TRNSYS: The transient energy system simulation tool. (2019). http://www.trnsys.com, accessed on Oct. 12, 2024.
[21] ASA FDM thermoplastic filament. https://support.stratasys.com/en/Materials/FDM/ASA, accessed on Oct. 12, 2024.
[22] F900: Stampante 3D FDM industriale. https://www.stratasys.com/it/3d-printers/printer-catalog/fdm/f900-printer/, accessed on Oct. 12, 2024.
[23] ISO 22007-2. (2015). Plastics-Determination of thermal conductivity and thermal diffusivity-Part 2: Transient plane heat source (hot disc) method. Switzerland.
[24] Hot Disk. (2022). Hot Disk thermal constants analyser instruction manual. Hot Disk, Sweden.
[25] Olcun, S., Ibrahim, Y., Isaacs, C., Karam, M., Elkholy, A., Kempers, R. (2023). Thermal conductivity of 3D-printed continuous pitch carbon fiber composites. Additive Manufacturing Letters, 4: 100106. https://doi.org/10.1016/j.addlet.2022.100106
[26] Islam, S., Bhat, G., Sikdar, P. (2023). Thermal and acoustic performance evaluation of 3D-Printable PLA materials. Journal of Building Engineering, 67: 105979. https://doi.org/10.1016/j.jobe.2023.105979
[27] Lopes, L., Reis, D., Paula Junior, A., Almeida, M. (2023). Influence of 3D microstructure pattern and infill density on the mechanical and thermal properties of PET-G Filaments. Polymers, 15(10): 2268. https://doi.org/10.3390/polym15102268
[28] Bute, I., Tarasovs, S., Vidinejevs, S., Vevere, L., Sevcenko, J., Aniskevich, A. (2023). Thermal properties of 3D printed products from the most common polymers. The International Journal of Advanced Manufacturing Technology, 124: 2739-2753. https://doi.org/10.1007/s00170-022-10657-7
[29] Laboratories. Università degli studi della Campania Luigi Vanvitelli. https://www.architettura.unicampania.it/dipartimento/strutture-del-dipartimento/laboratori/8-dipartimento/163-laboratories, accessed on Oct. 20, 2024.
[30] Zhao, D., Qian, X., Gu, X., Ayub Jajja, S., Yang, R. (2016). Measurement techniques for thermal conductivity and interfacial thermal conductance of bulk and thin film materials. Journal of Electronic Packaging, 138(4): 040802. https://doi.org/10.1115/1.4034605
[31] Köhl, M. (2007). Performance, durability and sustainability of advanced windows and solar components for building envelopes. Fraunhofer Institute for Solar Energy Systems. https://mojo.iea-shc.org/Data/Sites/1/publications/task27-b3.pdf, accessed on Oct. 12, 2024.
[32] Goia, F. (2016). Search for the optimal window-to-wall ratio in office buildings in different European climates and the implications on total energy saving potential. Solar Energy, 132: 467-492. https://doi.org/10.1016/j.solener.2016.03.031
[33] UNI. (2014). UNI TS 11300-1:2014 - Energy performance of buildings - Part 1: Evaluation of Energy need for space heating and cooling. Ente Nazionale Italiano di Unificazione (UNI).
[34] CEN. CEN/TC 228/WG 4 - Calculation methods and system performance and evaluation. CEN/TC 228 - Heating systems in buildings.
[35] Clint: Technical data sheet model CRA/K 15 -131. http://www.clint.it/, accessed on Oct. 12, 2024.
[36] Younes, C., Shdid, C.A., Bitsuamlak, G. (2011). Air infiltration through building envelopes: A review. Journal of Building Physics, 35: 267-302. https://doi.org/10.1177/1744259111423085
[37] Schimschar, S., Grözinger, J., Korte, H., Boermans, T., Lilova, V., Bhar, R. (2011). Panorama of the European non-residential construction sector. ECOFYS, Report to European Copper Institute.
[38] Ministero delle Imprese e del Made in Italy. (2015). Decreto interministeriale 26 giugno 2015 - Adeguamento linee guida nazionali per la certificazione energetica degli edifici. Governo italiano. https://www.mise.gov.it/index.php/it/normativa/decreti-

interministeriali/2032968-decreto-interministeriale-26-giugno-2015-adeguamento-linee-guida-nazionali-per-la-certificazione-energetica-degli-edifici, accessed on Oct. 12, 2024.
[39] Ciampi, G., Spanodimitriou, Y., Scorpio, M., Rosato, A., Sibilio, S. (2021). Energy performance of PVC-Coated polyester fabric as novel material for the building envelope: Model validation and a refurbishment case study. Journal of Building Engineering, 41: 102437. https://doi.org/10.1016/j.jobe.2021.102437
[40] Carlucci, S., Causone, F., De Rosa, F., Pagliano, L. (2015). A review of indices for assessing visual comfort with a view to their use in optimization processes to support building integrated design. Renewable and Sustainable Energy Reviews, 47: 1016-1033. https://doi.org/10.1016/j.rser.2015.03.062

NOMENCLATURE

ASA	Acrylonitrile Styrene Acrylate
Avg.	Average
CDA	Continuous Daylight Autonomy, %
COP	Coefficient of Performance (-)
E	Energy (kWh) / East
EER	Energy Efficiency Ratio (-)
EHP	Electric Heat Pump
EPS	Expanded PolyStyrene
FDM	Fused Deposition Modeling
h	Hours
HDD	Heating Degree Days
IEA	International Energy Agency
max	Maximum
min	Minimum
Of1	Office – part 1
Of2	Office – part 2
PC	Proposed Case
PES	Primary Energy Saving
RC	Reference Case
SSF	Second-Skin Façade
St	Stairs
T	Temperature
TPS	Transient Plane Source
TZ	Thermal zone
UDI	Useful Daylight Illuminance, %
UV	Ultraviolet
U-value	Transmittance value, W/m^2K
w	Windows
W	West
WWR	Windows-to-Wall Ratio, %

Greek symbols

α	Carbon dioxide equivalent emission factor for electricity production, $kgCO_{2,eq}/kWh_{el}$
Δ	Difference
η	Efficiency, %
λ	Thermal conductivity, W/mK

Subscripts

daylight	Natural light from the sun that illuminates spaces during daytime
useful	Range of daylight illuminance levels that are considered optimal for visual comfort
overlit	Percentage of time when daylight illuminance exceeds the upper limit
sensor	Sensor